RE-447J

PHOTOMETRIC AND POLARIMETRIC PROPERTIES OF THE BRUDERHEIM CHONDRITIC METEORITE

March 1973

RESEARCH DEPARTMENT

GRUMMAN AEROSPACE CORPORATION
BETHPAGE NEW YORK

Grumman Research Department Report RE - 447J

PHOTOMETRIC AND POLARIMETRIC PROPERTIES OF THE BRUDERHEIM CHONDRITIC METEORITE†

W. G. Egan[1]

J. Veverka[2]

M. Noland[2]

T. Hilgeman[1]

March 1973

[1]Research Department, Grumman Aerospace Corporation, Bethpage, New York, 11714.

[2]Laboratory for Planetary Studies, Cornell University, Ithaca, New York, 14850.

†Accepted for Publication in Icarus

Approved by: Charles E. Mack, Jr.

Charles E. Mack, Jr.
Director of Research

ABSTRACT

Photometric and polarimetric laboratory measurements were made as a function of phase angle in the U(0.36μm), G(0.54μm) and R(0.67μm) bands for 0^{o}, 30^{o} and 60^{o} incident illumination on four particle size ranges of Bruderheim, an L6 olivine-hypersthene chondritic meteorite. The four particle size ranges were: 0.25-4.76mm, 0.25-4.76mm coated with <74μm powder, 74-250μm, and < 37μm. In addition, normal reflectance measurments were made in the spectral range from 0.31 to 1.1μm. Comparison with astronomical data reveals that none of the asteroids in the main belt for which adequate observations exist can be matched with Bruderheim, which is representative of the most common meteoritic material encountered by the Earth. However, it appears from the polarization and photometry data that the surface of the Apollo asteroid Icarus is consistent with an ordinary chondrite composition. This suggests the possibility that this material, although common in Earth-crossing orbits, is rare as a surface constituent in the main asteroid belt.

I INTRODUCTION

Recently, much astronomical effort has been devoted to the study of the physical properties of asteroid surfaces. This has resulted in an ever growing store of spectral, photometric, and polarimetric data that have not been sufficiently complemented by laboratory measurements. Because there are many indirect arguments (Anders, 1964) which indicate that most meteorites are fragments of asteroid bodies, and since McCord, et al. (1970) have successfully identified the spectral reflectance curve of one asteroid, Vesta, with that of a basaltic achondrite, laboratory measurments on meteorite samples should prove useful in an intrepretation of asteroid surfaces. We have chosen to study the spectral, photometric, and polarimetric properties of the Bruderheim olivine-hypersthene chondrite, which is representative of the most common meteoritic material recovered on Earth (Mason, 1962), and, hence, might also be the most common in interplanetary space.

II INSTRUMENTATION

The Grumman goniometer, designed to measure the polarimetric and photometric properties of samples up to 60mm in diameter, consists of a light source on a 3-meter long arm and a sensor on another 3-meter long arm. The center of rotation of the arms is situated on the average sample surface, and the average normal to the surface lies in the plane defined by the arms.

The source is a G-E Type 2331 tungsten lamp, followed by a quartz ground glass diffuser, a Lyot depolarizer, an aperture plate, a 420 cycle, seven

bladed chopper, and an 11.4 cm diameter quartz objective lens. This assembly produces a beam collimated to 1^{o}, of uniform brightness to 1 percent or less, with a residual polarization of 0.1 percent or less on the 60mm illuminated sample area. The source arm is ordinarily fixed at an incident illumination angle between 0 and 60 degrees.

The sensors used in this investigation were photomultipliers RCA Types 6199 and 7102 with mumetal shields. The sensor arm normally traverses a phase angle range from 3.6 degrees to a maximum; at 0, 30, and 60 degrees incident illumination angles, the phase angle ranges are 3.6 to 65.5, 3.6 to 95.5 and 3.6 to 125.5 degrees, respectively. The sensor photometric system is axially symmetric, with an 11.4 cm diameter quartz objective lens, an aperture stop to limit the acceptance angle to 1 degree, a field lens to produce collimated light, followed by spectral filters and a rotating (6.5Hz) polarization analyzer. The residual polarization in the sensor system is less than 0.1%.

The spectral filters in the sensor system are of the type suggested by Gehrels and Teska (1960), and the system wavelength response has been determined experimentally. The U(0.36μm) analyses were made using the RCA 6199 (S-11) photomultiplier, an HNP'B polaroid, and a 3.0 mm thick Corning C-9863 filter. The infrared leak was found to be less than 2% of the observed signal levels for this filter-tube combination. The G(0.54μm) analyses were made using the RCA 6199 (S-11) photomultiplier, an HN-22 polaroid, a 3.0 mm thick Corning C-3385 filter, and a 2.0 mm thick Schott-Jena BG-18 filter. The R(0.67μm) analyses were made using the RCA 6199 (S-11) photomultiplier, an HN-22 polaroid, and a 3.0 mm thick Corning C-2030 filter.

The "normal" reflectance measurements were made at an incident angle of 0 degrees and a scattering angle of 3.6 degrees. Narrow band Optics

Technology interference filters were used between 0.31 and 0.7μm (at 0.02μm spacings to 0.4μm and at 0.03μm spacings above 0.4μm) with the RCA 6199 photomultiplier, and between 0.8 and 1.1μm (at 0.1μm spacings) with the RCA 7102 photomultiplier. The normal reflectances were calibrated against a freshly scraped magnesium carbonate surface. The relative reproducibility for each normal reflectance measurement is ±2%.

The polarimetric and photometric observations were phase detected using a Princeton Applied Research lock-in amplifier Type 124 and recorded on a Houston Instrument Omnigraphic Recorder. Polarimetric and photometric calibrations were made against $MgCO_3$ before and after each run.

The location of the polarization inversion angle is determined to an accuracy of $\pm 0.2^{\circ}$

III SAMPLES

The Bruderheim meteorite sample was obtained from Dr. E. Fireman of the Smithsonian Astrophysical Observatory. It is part of sample B-74 which was recovered within a day of the fall; weathering was minimal. The sample was subsequently stored in tightly closed bottles. The sample is representative of olivine-hypersthene meteorites (Keil and Fredriksson, 1964), and, more specifically, it is representative of class L6 (Tandon and Wasson, 1968). The black fusion crust was chipped off, and the remaining meteorite was fractured in a rock crusher to produce a minimum of small particles. The fracturing process was continued until there were no pieces larger than 4.76 mm. The fragments were then sieved in 5 minute runs using a Combs Gyratory Sifting Machine with sieves having openings of 4.76mm, 0.25mm, 74μm, 37μm, and a residual catch pan for <37μm. The first aim was to obtain enough material in the 0.25 to 4.76 mm particle size range to cover the 60 mm diameter sensing area of the goniometer. Then the remaining <0.25 mm particles were

subjected to further pulverization in a Coors 90 mm diameter porcelain mortar to obtain sufficient powder to coat the 0.25 to 4.76 mm particles.

The 0.25 to 4.76 mm sample, weighing 42 grams, is shown in Figure 1a. The particles are plate-like, with angular edges, and tend to lie flat. Figure 1b shows the microscopic appearance of a typical fragment; chondrules and bits of nickel-iron are clearly visible.

Next, the "coated" sample (Figure 1c) was made by dusting the 0.25 to 4.76 mm sample with 0.87 g of the <37μm powder, and 0.12g of the 37-74μm powder. The coating amounted to 2.4% by weight. A microscopic view of this sample is shown in Figure 1d.

After these two coarse samples were measured, two other samples were prepared by further crushing in the mortar: 75-250μm (Figure 1e), and <37μm (Figure 1f). The latter sample has the expected "fairy castle" texture.

IV NORMAL REFLECTANCE MEASUREMENTS

The absolute normal reflectance of the four samples is shown in Figure 2. As mentioned above, these "normal" reflectance measurements were actually made with an incident angle of 0 degrees and an emission angle of 3.6 degrees. No correction to convert these measurements to precisely zero phase was attempted.

As expected, of the two powders the <37μm sample is brighter than the 74-250μm sample throughout our spectral range. The "coated" sample has a curve intermediate to those of the two powders, as it should, since it was produced by dusting the 0.25-4.76 mm sample with a coating of particles smaller than 74μm. Incidentally, this illustrates the fact that for a sample of large particles that have been completely coated with smaller particles, the inherent photometric properties of the large

particles are suppressed.

The spectral reflectance curve of the 0.25-4.76mm sample seems anomalous. Its shape differs from that of the other curves, it crosses the "coated" sample curve at 0.6μm, and it is higher than the 74-250μm curve. Intuitively, one would not expect the coated sample curve to fall below that for the 0.25 to 4.76 mm sample because the addition of fine particles should increase the importance of multiple scattering and, therefore, the brightness of the sample. We do not understand this anomalous behaviour, but it may possibly be related to the presence of quasi-planar facets (Figure 1a).

The 0.25 to 4.76mm sample shows three distinct absorption features, two strong bands near 0.3μm and 0.95μm, both due to Fe^{2+} (Bancroft and Burns, 1967; White and Keester, 1967), and a weak feature near 0.6μm that usually is attributed to Fe^{3+} (Hunt and Salisbury, 1970). In the case of Bruderheim, Egan and Hilgeman (1972) have shown this absorption feature to be due to FeS.

The 0.6μm band is not evident in the spectra of the other samples. The ferrous 0.3μm feature is generally similar in all the samples while that at 0.95μm shows definite variations. The relative depth (minimum over maximum brightness in percent subtracted from one hundred) is 15, 40, 25 and 30 percent for the <37μm, 74-250μm, "coated" and 0.25-4.76mm samples, respectively. It is reasonable that the band is deeper for the 74-250μm sample than for the <37μm sample, and that the depth is intermediate for the "coated" aample. However, one would expect the 0.25 to 4.76mm sample to have the deepest band, which is not the case. This is another indication that the reflectance curve for this sample is anomalous.

V PHOTOMETRIC MEASUREMENTS

Photometric measurements were made as a function of phase angle in the U(0.36μm), G(0.54μm) and R(0.67μm) bands, for 0^{o}, 30^{o} and 60^{o} incident illumination angle on the four particle size samples of Bruderheim. We have chosen to present these data in two ways: first, in terms of the usual phase curve which gives the brightness (here normalized to that at a phase of 3.6^{o}) as a function of the phase angle (B-curve); and in terms of a function which minimizes the effects of geometry (f-curve).

For a particulate surface in which multiple scattering is small, the intensity of the scattered light can be represented by an equation of the following type (Irvine, 1966; Veverka, 1970):

$$B(i,\epsilon,\alpha) \sim \tilde{\omega}_o \left\{\frac{\cos i}{\cos i + \cos \epsilon}\right\} \cdot f(i,\epsilon,\alpha) \qquad (1)$$

where $\tilde{\omega}_o$ is the single particle scattering albedo, and i, ϵ, α are the incidence, scattering, and phase angles, respectively. Here, f is a complicated function that depends on the phase function of a single particle and on the texture of the surface.

When Eq. (1) is strictly applicable, that is when, among other things, multiple scattering is negligible, then f does not depend strongly on i or ϵ individually, but only on the phase angle α. In that case, Eq. (1) is approximated by

$$B(i,\epsilon,\alpha) \sim \tilde{\omega}_o \left\{\frac{\cos i}{\cos i + \cos \epsilon}\right\} \cdot f(\alpha). \qquad (2)$$

This is analogous to the lunar photometric function derived semi-empirically by Hapke (1963; 1965); when $f(\alpha)$ = constant, independent of phase

angle, Eq. (2) reduces to the Lommel-Seeliger law.

The real photometric information about a surface is contained in the f-function. In the usual phase curve (B-plot), this information is obscured by the purely geometrical factor $\{\cos i/(\cos i + \cos \epsilon)\}$ which is, of course, the same for all surfaces. It is for this reason that we have chosen to present our photometric results in terms of both B-plots, that are astronomically more convenient, and f-plots, that are physically more informative.

The photometric characteristics of the four samples are shown in Figs. 3,4,5 and 6, and summarized in Tables I, II, III, and IV. The figures show both the B-curves and the f-curves, as well as the color dependence of the f curves at each of the three incidence angles studied (0°, 30°, 60°). For instance, Δf_{30} give the (U-G) and (G-R) magnitude differences in the f function at an incident angle of 30 degrees (Note that $\Delta f \equiv \Delta B$).

For the 74 to 250μm, and the "coated" sample (Figs. 5 and 4), the f-function is truly independent of i, and is only a function of the phase angle α. This indicates that multiple scattering is not dominant in these two samples. For the <37μm sample, the f-function shows a small dependence on the angle of incidence, especially at large phase angles (Fig. 6), probably due to the increased importance of multiple scattering. The f-function for the 0.25 to 4.76 mm sample (Figure 3) shows some dependence on i at all phase angles. This is not surprising because this sample consists of coarse, plate-like chips, and Eq. (1) cannot be applied strictly (Veverka, 1970).

Most of the samples get redder with increasing phase. This is a common property of silicate powders discussed by Adams and Filice (1967), who also found that this trend often reverses at large phase angles (powders becoming bluer with increasing phase). There are indications of this happening in some of our samples at phase angles larger than 70°. The coarse sample, however, is anomalous in this respect. The (U-G) color index shows a reddening with phase, but the (G-R) index does not (Fig. 3).

In terms of astronomical applications we are most interested in the photometric properties up to phase angles of about 30°, because for asteroids, larger phase angles are not normally observable from Earth. Therefore, using the above curves we have evaluated the following parameters:

a) the phase coefficient (for either B-curves, or f-curves), defined to be the slope of the curve between 10° and 30°.

b) the opposition effect, defined here to be the difference in magnitude between the actual brightness at $\alpha = 3.6^{\circ}$, and that inferred by extrapolating to this value from $\alpha = 10^{\circ}$, using the phase coefficient.

These parameters are tabulated for the various samples in Tables I, II, III, and IV. The magnitudes of the phase coefficients and their color dependence are typical of samples of such texture and reflectance. The values of the opposition effect given in Tables I, II, III, and IV, are estimates, as our measurements were not optimized to study this parameter. Other things being equal, the opposition effect for the powder and

"coated" samples is largest at the shortest wavelengths where the albedo is the lowest. This is reasonable because multiple scattering hinders shadowing, and therefore, weakens opposition effects. Also, the <37μm and 74 to 250μm sample have more pronounced opposition surges than the other two samples, in accordance with their more intricate microscopic texture (Fig. 1).

VI POLARIZATION MEASUREMENTS

For each sample, polarization measurements were made in the U, G, and R as a function of phase angle for incidence angles 0°, 30° and 60°. These results are shown in Figs. 7, 8, 9 and 10, and are summarized in Tables V, VI, VII, and VIII.

As first noted by Lyot (1929), one should expect the magnitude of the positive branch to be inversely correlated with sample albedo. This is because an increase in the importance of multiple scattering within a sample increases the albedo and decreases the polarization. This trend is present in our measurements. Both the amount of polarization at $\alpha = 60^{\circ}$, and h, the slope of the positive branch near the cross-over angle, tend to show an inverse correlation with surface reflectance (Tables V, VI, VII and VIII).

The dependence of the positive branch on sample texture and color is indirect, in that texture and color seem to be important only to the extent that they affect the reflectance of the sample.

Up to phase angles of about 60°, the dependence of the polarization curves on incidence angle is small, in all colors, and for all samples. To first order, the polarization curves are functions of α only, and do

not depend strongly on i or ϵ separately. Only for the coarse sample does the dependence on i become strong, and then only at large phase angles (Fig. 7). This is probably due to the fact that the flat, almost flake-like, particles of this sample (Fig. 1a), tend to scatter quasi-specularly at large phase angles.

What are the effects of albedo, color and scattering geometry on the negative branch? To first order, the negative branch depends only on the phase angle, and not on i or ϵ separately (Tables V, VI, VII and VIII). The depth of the negative branch does not appear to vary systematically with either color or albedo. This is also true for the angle of minimum polarization, α_{min}. The cross-over angle, α_x, appears to be inversely correlated with particle size (Comparing Tables VII and VIII), and thus directly correlated with albedo (and consequently with wavelength). This is in contrast to observations by Egan (1967) of Haleakala volcanic ashes and a furnace slag, which showed an opposite trend in this particle size range.

VII APPLICATION TO ASTEROID ASTRONOMY

An important astronomical task is to attempt to identify, if possible, the asteroid parent body of the Bruderheim chondrite. Three types of information are at our disposal: the spectral reflectance curves (Sec. IV), the photometric phase curves (Sec. V) and the polarization curves (Sec. VI).

The spectral reflectance measurements are of primary importance for two main reasons: first, they are in many cases diagnostic of composition (Adams, 1968; McCord et al., 1970), and secondly, there is no serious

difficulty in going from proper laboratory measurements to disk integrated values. This latter advantage is shared by the polarization measurements, because as Figs. 7, 8, 9, and 10 show, at small phase angles the degree of polarization would be roughly uniform across the disk. Polarization curves contain important information about the texture of the surface and its albedo, but are much less diagnostic of composition (Veverka, 1970) than spectral reflectance curves.

The photometric phase curves are the most difficult to use diagnostically. First, asteroid observations involve disk integrated quantities, whereas, laboratory measurements simulate conditions at only a single point on the disk. Thus, an integration of the photometric function over the disk is required before any comparison with asteroid observations can be made. Even then there are complications as the phase coefficients may be significantly altered by large-scale surface roughness (Veverka, 1971a) in a way which cannot be uniquely determined from the observations. In other words, phase coefficients calculated on the basis of laboratory measurements can only be compared with asteroids whose surfaces do not have significant large-scale roughness. Secondly, there is no evidence to indicate that phase coefficients, or their color dependence, are diagnostic of composition. As a result, photometry becomes relevant only if the spectral reflectance curves of Bruderheim can first be successfully matched with those of some asteroid. Then it is possible to use the data in Sec. V, to construct phase coefficients for the disk integrated light, assuming various degrees of surface roughness (Veverka, 1971a), in order to check that these also agree with observations.

Thus, a reasonable plan of attack in trying to simulate asteroid observations with laboratory measurements is the following:

1) Verify agreement of the spectral reflectance curve.

2) Determine if polarization curves are compatible.

3) Check that the photometric properties of the material are consistent with those of the asteroid.

We shall now use this procedure to see if there are asteroids whose surface composition is comparable to Bruderhiem. The most extensive study of asteroid spectral reflectance curves is that of Chapman (1972). Of the 32 asteroids analysed by Chapman, only Vesta has a spectral reflectance curve at all similar to Bruderheim (Fig. 11a). However, on the basis of more detailed study of the location and shape of the band near 1μm, McCord et al. (1970) have concluded that this spectrum is better matched by a basaltic achondrite than by an ordinary hypersthene-olivine chondrite such as Bruderheim. In fact, even though the closest match with our data occurs for the <37μm Bruderheim powder, there is a distinct discrepancy in the near infrared, where the <37μm powder is too dark by about 25% at 1.1μm. Also shown in Fig. 11a are the spectral reflectance curves for Juno and Hebe, both of which show absorption bands in the UV and near 1μm, but which do not match the shape of the Bruderheim spectra. Many other asteroids such as Ceres and Pallas have spectra that are not at all similar to that of Bruderheim.

Polarization curves are available for about a dozen asteroids (Veverka, 1970, 1971b, 1971c). Because very few asteroids can be observed from Earth at phase angles larger than about 30 degrees, the characteristics of the negative branch (depth, angle of minimum polarization, and inversion angle) must serve as the primary comparison criteria. Generally speaking,

asteroid negative branches are deeper and inversion angles larger than those for Bruderheim material. The one exception is Vesta, whose polarization curve is somewhat similar to that of Bruderheim.

It is noteworthy that the spectral reflectance curve of Icarus, an earth-crossing asteroid, bears some resemblance to Bruderheim (Fig. 11b). These data are taken from Gehrels et al. (1970), and are difficult to compare rigorously with our measurements as they were made using wide-band filters. To strengthen the argument, the polarization curve of Icarus is consistent with the curves for Bruderheim (Gehrels et al, 1970). As Icarus was only observed over phase angles ranging from 40° to 100°, its negative branch cannot be compared with those of our samples, but at $\alpha = 60^{\circ}$ the polarization of Icarus is about 3.5% (in the spectral range of our G filter) that compares favorably with the values for the "coated" sample given in Table VI.

VIII DISCUSSION AND CONCLUSIONS

Bruderheim is a sample of an ordinary olivine-hypersthene chondrite, and as such is supposedly representative of the most common meteorite type which falls to Earth. Therefore, unless the distribution of meteoroids by composition is very heterogeneous in space, Bruderheim should be representative of one of the most common meteorite types in the solar system. Of all the asteroids studied to date, however, only Icarus and Vesta resemble Bruderheim, and the similarity to Vesta is only qualitative (Sec. VII). Of the many asteroid spectral curves which have an absorption band near 1μm (for example Juno and Hebe), none match exactly, as this band is never deep enough (Fig. 11a).

There are at least two possibilities: first, most of the asteroids observed are composed of ordinary olivine-hypersthene chondritic material, but the details of the spectral reflectance curves (such as the depth of the 1μm band) are selectively modified by some process to produce the observed variations; secondly the surfaces of most asteroids in the belt do not consist of such material. The latter alternative has obvious important implications.

Consider the first alternative. A number of processes can modify the spectral reflectance curves so as to decrease the relative depth of the 1μm band. These include: "solar wind darkening" (Hapke and van Horne, 1963; Ken Knight et al. 1967; Wehner et al, 1963), decrease of mean particle size (Adams, 1968), and contamination with other materials, including dark glass derived from hypervelocity impacts (Adams and McCord, 1971, 1972). No matter which process is invoked, it must allow for the fact that Icarus and Vesta remain unaffected, and this we believe is impossible to acheive. Icarus and Vesta are on opposite ends of the asteroid size spectrum; consequently, any explanation based on size, such as the ability to retain a regolith, must be ruled out. Also, because Vesta, like Juno and Hebe, is a main belt asteroid, an explanation based on differences in orbital environment seems unlikely. Space weathering is hard to reconcile with the fact that the spectrum of Vesta has been successfully matched with that of a basaltic achondrite. Another process to be considered is that the Bruderheim meteorite has suffered substantial alteration since it fell to earth; however, as discussed in Section III, we feel that this is quite unlikely. Finally, it could be argued that the infrared portions of published asteroid spectral reflectance curves have a systematic error. However, not only does the data show internal

consistency, but the instrumentation used by Chapman has been employed in many applications where this type of error would have been obvious. Thus, we must seriously consider the alternative hypothesis: none of the main belt asteroids studied to date consist of ordinary chondritic material.

It is certainly possible that the sample of meteorites intercepted by the Earth need not be compositionally representative of the bulk of the asteroid belt. In fact, there is strong evidence, both chemical (Anders, 1964) and orbital (Anders, 1971) that most meteorites are derived from a small number (probably less than a dozen) of parent bodies. An interesting possibility is that some of the Apollo asteroids, such as Icarus, may consist of ordinary chondritic material of this type, and that this material, although rare as a surface constituent of large asteroids in the main belt, is very common in Earth-crossing orbits.

The conclusions in this paper are based on one chondritic meteorite, more specifically of the L6 class. This does not mean that the results apply to a less metamorphosed sample (eg. of the L3 class). These results are presented with this caution in mind. Clearly further detailed studies of chondritic meteorites are highly desirable.

Acknowledgement:

We wish to thank E. Fireman of the Smithsonian Astrophysical Observatory for the Bruderhiem meteorite sample, and C. Sagan, F. Whipple, and L. Wasserman for indispensable assistance. This study was supported in part by the Grumman Aerospace Corporation, and in part by NASA Grant NGR- 33-010-082, to the Laboratory of Planetary Studies, Cornell University. We also wish to thank E. Anders for helpful comments on an earlier version of this manuscript.

REFERENCES

Adams, J.B. (1968). Lunar and Martian surfaces: Petrologic significance of absorption bands in the near-infrared. Science 159, 1453 - 1455.

Adams, J.B. and Filice, A.L. (1967). Spectral reflectance 0.4-2.0μ of silicate rock powders. J. Geophys. Res., 72, 5705 - 5715.

Adams, J.B. and McCord, T.B. (1971). Alteration of lunar optical properties: Age and composition effects. Science, 171, 567 - 571.

Adams, J.B. and McCord, T.B. (1972). Optical evidence for regional cross-contamination of highland and mare soils, 3rd Lunar Science Conference (Abstracts), Lunar Science Institute and NASA Manned Spacecraft Center, Houston, Texas, January 10-13, 1972, pp. 1-3.

Anders, E. (1964). Origin, age and composition of meteorites. Space Sci. Rev., 3, 583 - 714.

Anders, E. (1971). Interrelations of meteorites, asteroids, and comets. Physical Studies of Minor Planets. NASA SP-267 (T. Gehrels, ed.), pp. 429 - 446.

Bancroft, G. M. and Burns, R. G. (1967). Interpretation of the electronic spectra of iron in pyroxenes. American Mineralogist 52, pp. 1278-1287.

Chapman, C. R. (1972). Surface properties of asteroids. Ph.D. Thesis, MIT, Cambridge, Mass.

Egan, W. G. (1967). Polarimetric measurements of lunar surfaces, J. Geophys. Res., 72, 3233 - 3245.

Egan, W. G. and Hilgeman, T. (1972). Fundamental optical properties of the Bruderheim meteorite. Bulletin A.A.S. 4, 425.

Gehrels, T. and Teska, T.M. (1960). A Wollaston photometer, Publ. Astron. Soc. Pacific, 72, 115 - 122.

Gehrels, T., Roemer, E., Taylor, E. C. and Zellner, B. H. (1970). Minor planets and related objects. IV. Asteroid (1566) Icarus. Astron. J. 75, 186 - 195.

Hapke, B. W. (1963). A theoretical photometric function for the lunar surface. J. Geophys. Res., 68, 4571 - 4586.

Hapke, B. W. (1966). An improved theoretical lunar photometric function. Astron. J. 73, 333 - 339.

Hapke, B. W. and Van Horn, H. (1963). Photometric studies of complex surfaces, with applications to the Moon. J. Geophys. Res., 68, 4545 - 4570.

Hunt, G.R. and Salisbury, J.W. (1970). Visible and near-infrared spectra of minerals and rocks: I. Silicate minerals. Modern Geology, 1, 283 - 300.

Irvine, W.M. (1966). The shadowing effect in diffuse reflection, J. Geophys. Res., 71, 2931 - 2937.

Keil, K. and Fredriksson, K. (1964). The iron, magnesium and calcium distribution in coexisting olivines and rhombic pyroxenes of chondrites, J.G.R. 69, pp. 3487 - 3515.

Ken Knight, E. C., Rosenberg, D.L., and Wehner, G.K. (1967). Parameters of the optical properties of the lunar surface powder in relation to solar wind bombardment, J. Geophys, Res., 72, 3105 - 3129.

Lyot, B. (1929). Research on the polarization of light from planets and some terrestrial substances. Annales de l'Observatoire de Paris, Secion de Meudon, VIII, No. 1, 161 pp. Also NASA Technical Translation TTF-187.

Mason, B. (1962). Meteorites, pp. 91 - 92, Wiley, New York.

McCord, T.B., Adams, J.B. and Johnson, T.V. (1970). Asteroid Vesta: spectral reflectivity and compositional implications, Science, 168, 1445 - 1447.

Tandon, S. N. and Wasson, J. T. (1968). Gallium, germanium, indium and iridium variations in a suite of L-group chondrites, Geochimica et Cosmochimica Acta, 32, pp. 1087 - 1109.

Veverka, J. (1970). Photometric and polarimetric studies of minor planets and satellites. Ph.D. Thesis, Harvard University, Cambridge, Mass.

Veverka, J. (1971a). The physical meaning of phase coefficients. Physical Studies of Minor Planets NASA SP-267. (T. Gehrels, ed) pp. 79 - 90.

Veverka, J. (1971b). Asteroid polarimetry: A progress report. Physical Studies of Minor Planets NASA SP-267. (T. Gehrels, ed), pp. 91 - 94.

Veverka, J. (1971c). The polarization curve and absolute diameter of Vesta. Icarus, 15, 11 - 17.

Wehner, G.K., Ken Knight, C.E. and Rosenberg, D. (1963). Modification of the lunar surface by solar wind bombardment. Planet Sp. Science, 11, 1257 - 1261.

White, W. B. and Keester, K. L. (1967). Selection rules and assignments for the spectra of ferrous iron in pyroxenes. American Mineralogist, 52, pp. 1508 - 1544.

Color	Angle of Incidence (deg)	Reflectance at $\epsilon = 0^{o}$ $i = 3.6^{o}$	f at $\alpha = 60^{o}$	Phase Coefficient (B-curve) (mag/deg)	Phase Coefficient (f-curve) (mag/deg)	Opposition Effect Δm (B-curve)
U	0	.21	0.77	.007	.010	.04
	30	.20	0.63	.012	.011	.05
	60	.16	0.54	.019	.009	.04
G	0	.24	0.66	.007	.010	.04
	30	.23	0.58	.011	.009	.05
	60	.16	0.46	.018	.008	.02
R	0	.25	0.68	.007	.010	.05
	30	.23	0.62	.011	.009	.06
	60	.16	0.48	.017	.007	.05

Table I: Photometric Properties of the 0.25-4.76mm Sample

Color	Angle of Incidence (deg)	Reflectance at $e = 0^{\circ}$ $i = 3.6^{\circ}$	f at $\alpha = 60^{\circ}$	Phase Coefficient (B-curve) (mag/deg)	Phase Coefficient (f-curve) (mag/deg)	Opposition Effect Δm (B-curve)
U	0	.20	0.74	.010	.013	.05
	30	.18	0.69	.015	.013	.07
	60	.14	0.66	.023	.013	.05
G	0	.24	0.62	.009	.012	.02
	30	.23	0.61	.013	.011	.04
	60	.17	0.59	.021	.011	.05
R	0	.25	0.61	.008	.011	.03
	30	.24	0.59	.012	.010	.05
	60	.18	0.55	.021	.011	.04

Table II: Photometric Properties of the "coated" Sample

Color	Angle of Incidence (deg)	Reflectance at $\varepsilon = 0^{o}$ $i = 3.6^{o}$	f at $\alpha = 60^{o}$	Phase Coefficient (B-curve) (mag/deg)	Phase Coefficient (f-curve) (mag/deg)	Opposition Effect Δm (B-curve)
U	0	.18	0.55	.005	.008	.06
	30	.17	0.45	.010	.009	.06
	60	.14	0.44	.018	.010	.11
G	0	.22	0.40	.004	.007	.05
	30	.20	0.37	.008	.006	.05
	60	.16	0.34	.016	.007	.08
R	0	.23	0.37	.003	.007	.05
	30	.21	0.34	.008	.006	.05
	60	.16	0.29	.015	.006	.07

Table III: Photometric Characteristics of the 74-250μm Sample

Color	Angle of Incidence (deg)	Reflectance at $\epsilon = 0^{\circ}$ $i = 3.6^{\circ}$	f at $\alpha = 60^{\circ}$	Phase Coefficient (B-curve) (mag/deg)	Phase Coefficient (f-curve) (mag/deg)	Opposition Effect Δm (B-curve)
U	0	.22	0.49	.004	.008	.04
	30	.20	0.34	.009	.007	.07
	60	.17	0.38	.017	.008	.10
G	0	.26	0.35	.003	.006	.04
	30	.24	0.28	.008	.006	.02
	60	.19	0.26	.015	.005	.08
R	0	.27	0.35	.003	.006	.04
	30	.26	0.26	.006	.005	.04
	60	.19	0.23	.014	.004	.08

Table IV: Photometric Characteristics of the < 37 μm Sample

Color	Angle of Incidence (deg)	Reflectance at $\epsilon = 0^{o}$ $i = 3.6^{o}$	Polarization at $\alpha = 60^{o}$ (%)	h (%/deg)	Inversion Angle (deg)	Minimum Polarization (%)	Angle of Minimum Polarization (deg)
U	0	.21	+6.6	.12	15.3	-0.5	7.0
	30	.20	+6.0	.10	17.2	-0.5	5.5
	60	.16	+5.8	.09	16.5	-0.7	8.0
G	0	.24	+5.2	.09	15.8	-0.6	4.5
	30	.23	+4.8	.08	16.7	-0.4	3.5
	60	.16	+4.7	.09	16.2	-0.6	7.0
R	0	.25	+4.8	.08	16.0	-0.4	3.5
	30	.23	+4.8	.08	18.4	-0.5	3.5
	60	.16	+4.0	.07	17.4	-0.4	3.5

Table V: Polarization Characteristics of the 0.25-4.76mm Sample

Color	Angle of Incidence (deg)	Reflectance at $\epsilon = 0^{\circ}$ $i = 3.6^{\circ}$	Polarization at $\alpha = 60^{\circ}$ (%)	h (%/deg)	Inversion Angle (deg)	Minimum Polarization (%)	Angle of Minimum Polarization (deg)
U	0	.20	+4.3	.08	13.6	-0.2	3.5
	30	.18	+4.4	.09	15.1	-0.3	3.5
	60	.14	+4.8	.09	15.6	-0.4	3.5
G	0	.24	+3.1	.08	14.3	-0.3	3.5
	30	.23	+3.1	.06	14.7	-0.3	3.5
	60	.17	+3.3	.08	16.7	-0.4	5.5
R	0	.25	+2.8	.05	13.7	-0.3	3.5
	30	.24	+2.8	.05	15.8	-0.2	3.5
	60	.18	+3.0	.07	17.5	-0.3	3.5

Table VI: Polarization Characteristics of the "coated" Sample

Color	Angle of Incidence (deg)	Reflectance at $\epsilon = 0^{\circ}$ $i = 3.6^{\circ}$	Polarization at $\alpha = 60^{\circ}$ (%)	h (%/deg)	Inversion Angle (deg)	Minimum Polarization (%)	Angle of Minimum Polarization (deg)
U	0	.18	+6.2	.12	15.7	-0.5	3.5
	30	.17	+6.6	.11	15.9	-0.4	3.5
	60	.14	+6.7	.12	16.0	-0.5	3.5
G	0	.22	+4.4	.09	15.1	-0.4	3.5
	30	.20	+4.8	.09	15.1	-0.4	3.5
	60	.16	+4.9	.10	16.8	-0.5	3.5
R	0	.23	+4.2	.09	15.4	-0.5	3.5
	30	.21	+4.7	.09	15.8	-0.5	3.5
	60	.16	+4.6	.09	17.7	-0.5	3.5

Table VII: Polarization Characteristics of the 74-250μm Sample

Color	Angle of Incidence (deg)	Reflectance at $\epsilon = 0^\circ$ $i = 3.6^\circ$	Polarization at $\alpha = 60^\circ$ (%)	h (%/deg)	Inversion Angle (deg)	Minimum Polarization (%)	Angle of Minimum Polarization (deg)
U	0	.22	+3.4	.07	16.5	-0.3	7.0
	30	.20	+3.4	.07	17.0	-0.4	4.5
	60	.17	+3.5	.07	19.3	-0.4	7.5
G	0	.26	+2.4	.05	17.0	-0.3	3.5
	30	.24	+2.6	.05	17.0	-0.4	7.0
	60	.19	+2.6	.05	18.3	-0.4	3.5
R	0	.27	+2.3	.05	17.0	-0.4	7.0
	30	.26	+2.4	.05	17.5	-0.4	7.3
	60	.19	+2.4	.05	20.3	-0.5	7.5

Table VIII: Polarization Characteristics of the < 37μm Sample.

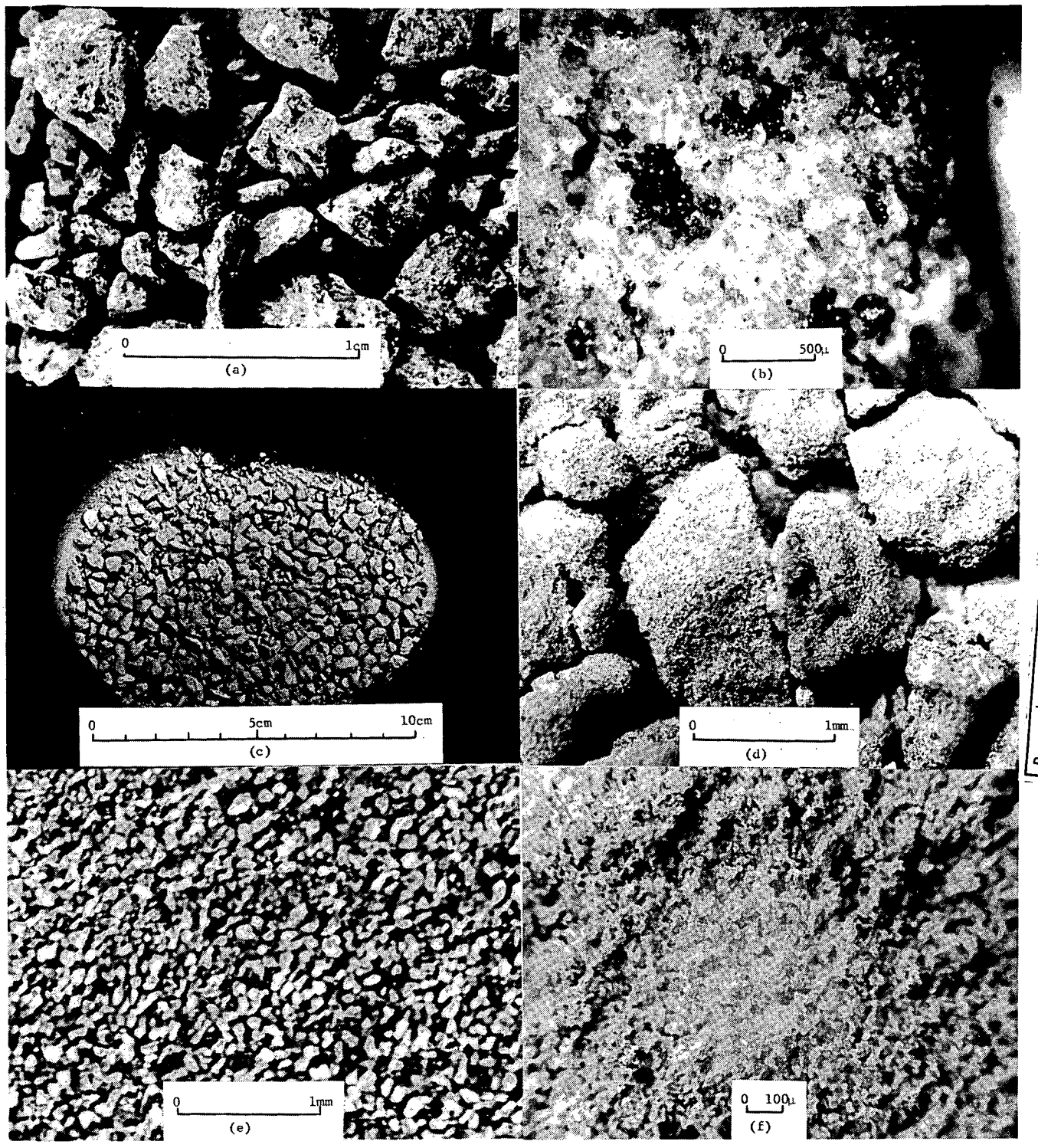

Fig. 1 Photographs of the Bruderheim Meteorite Samples. a) 0.25 to 4.76 mm particulates; b) microscopic view of 0.25 to 4.76 mm particulates; c) "coated" particulates; d) microscopic view of "coated" particulates; e) 74 to 250 μm grains; f) < 37 μm powder

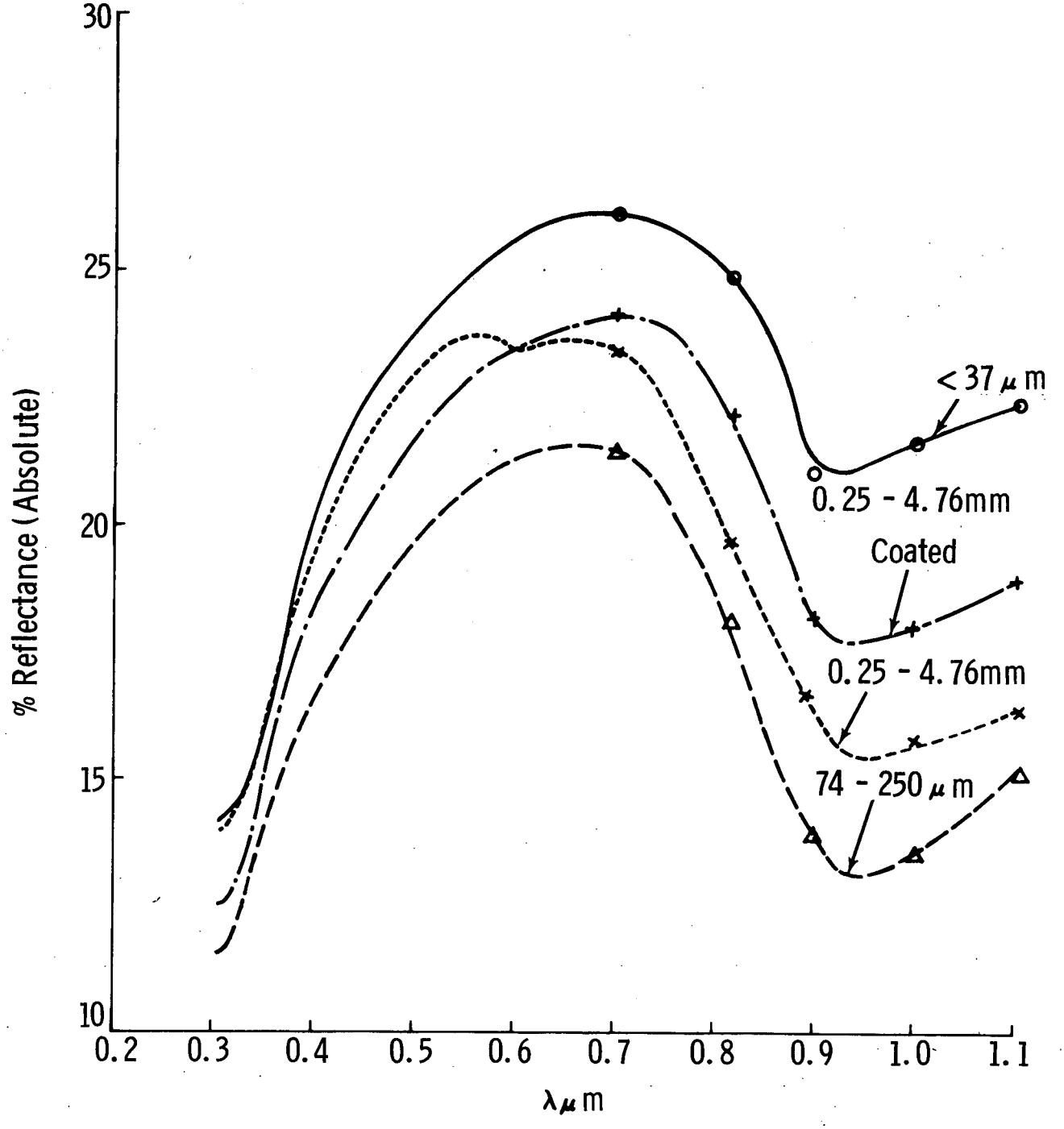

Fig. 2 Absolute Normal Reflectance of the Bruderheim Meteorite Samples. (Data points are shown between 0.7 and 1.1 μm; points below 0.666 μm measured at intervals $\leq$ 0.03 μm are omitted for clarity.)

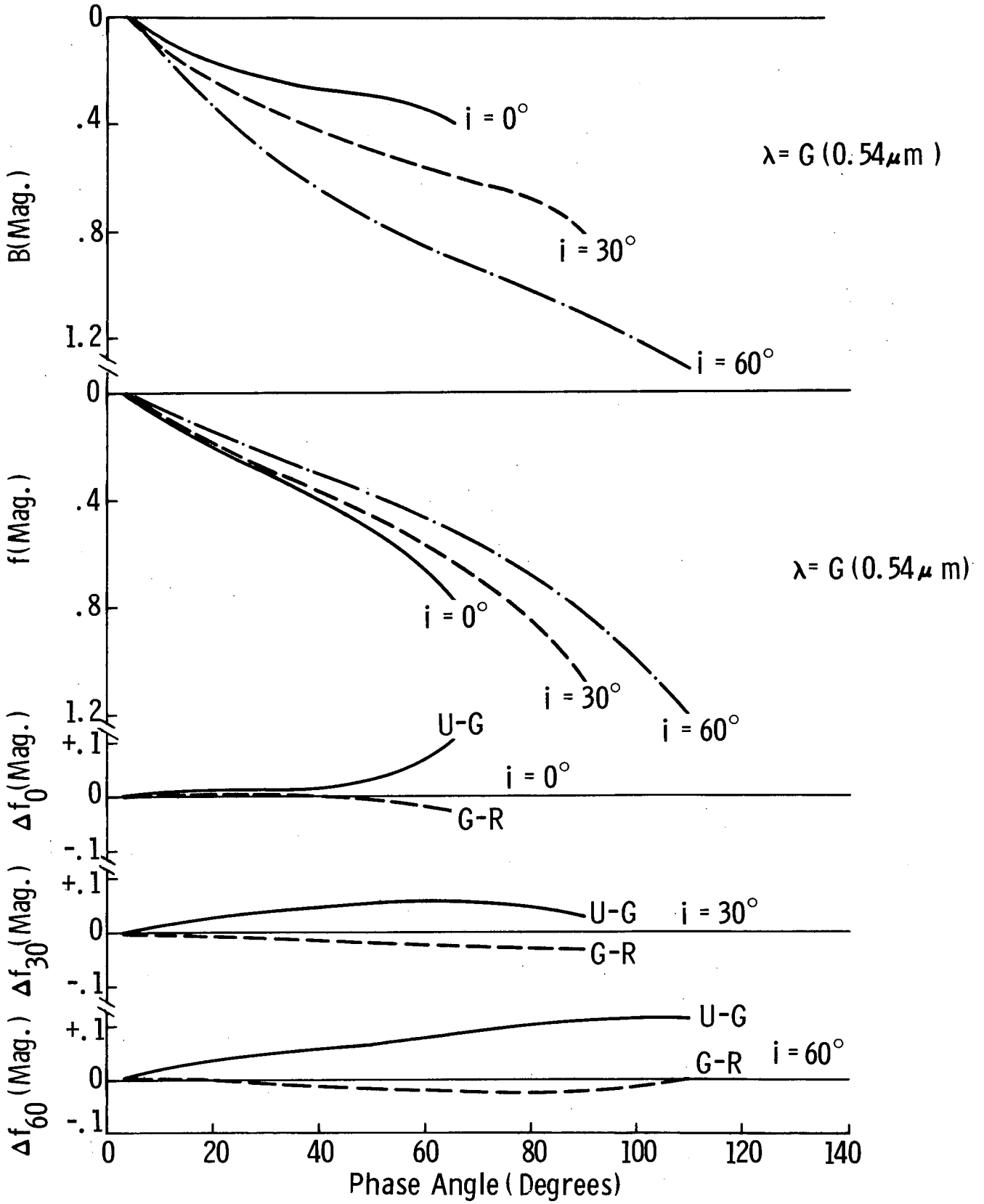

Fig. 3 Photometric Properties of 0.25 to 4.76 mm Bruderheim Particulates

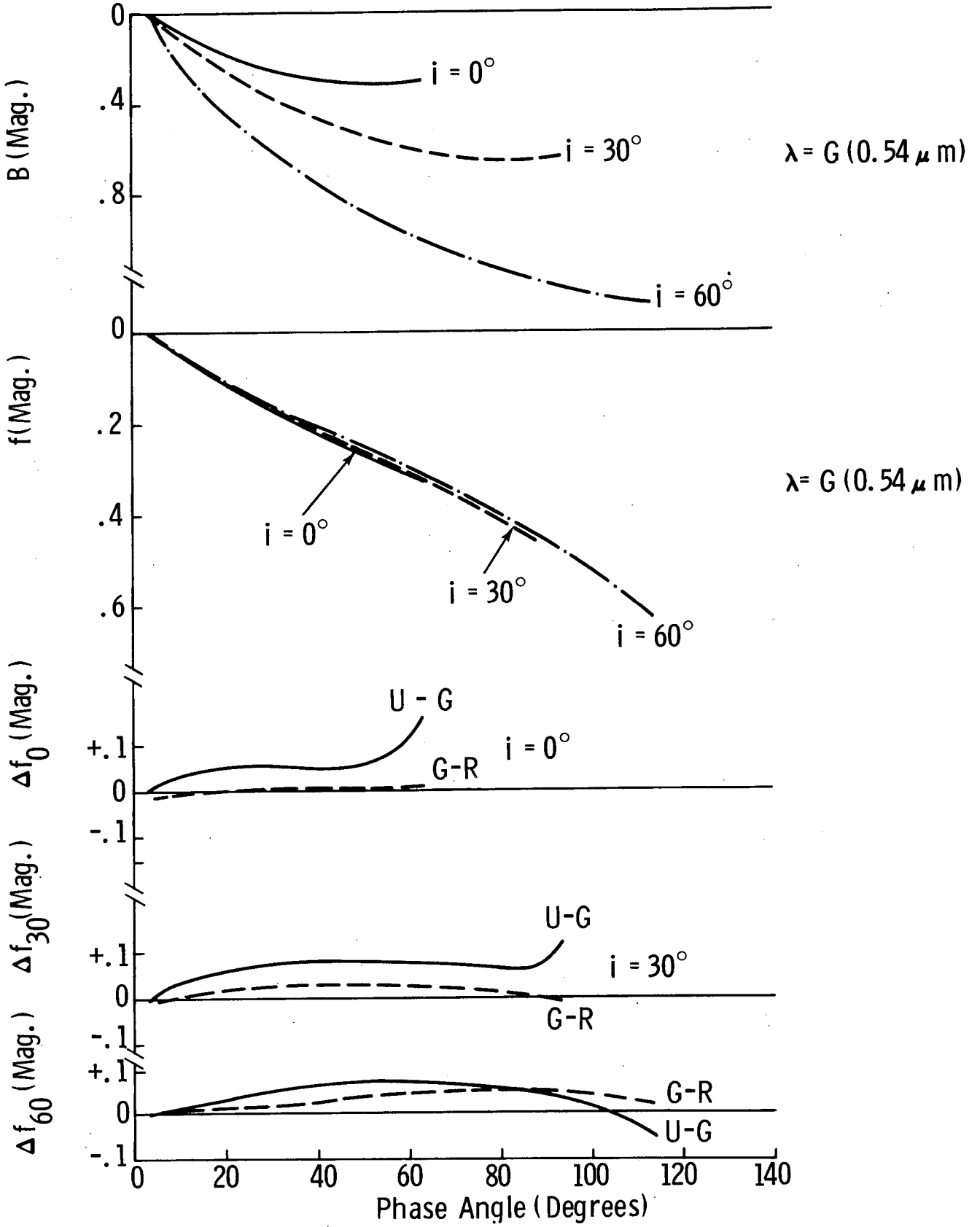

Fig. 4 Photometric Properties of 0.25 to 4.76 mm Bruderheim Particulates Coated with < 74 μm Bruderheim Powder

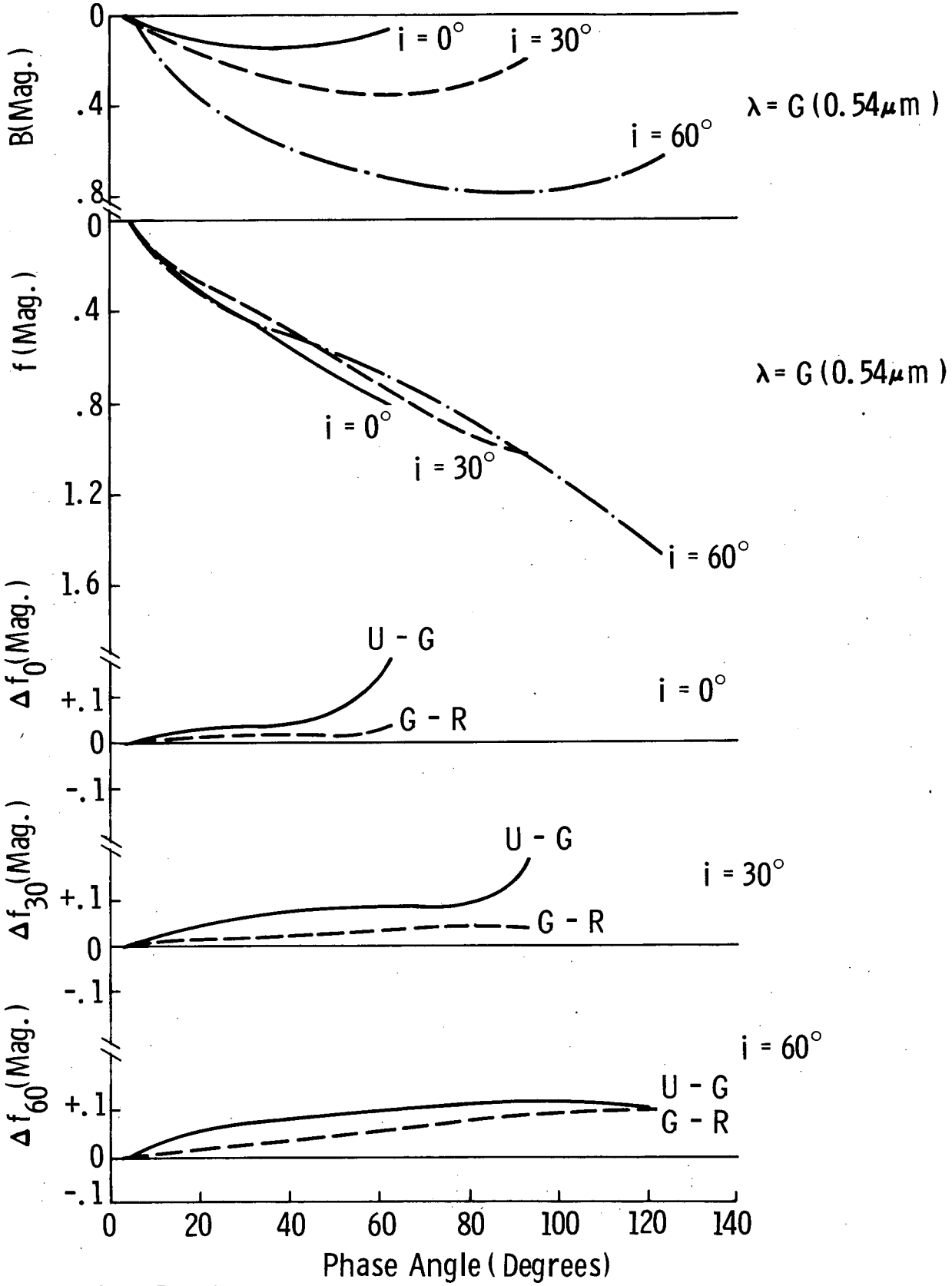

Fig. 5 Photometric Properties of 74 to 250 μm Bruderheim Grains

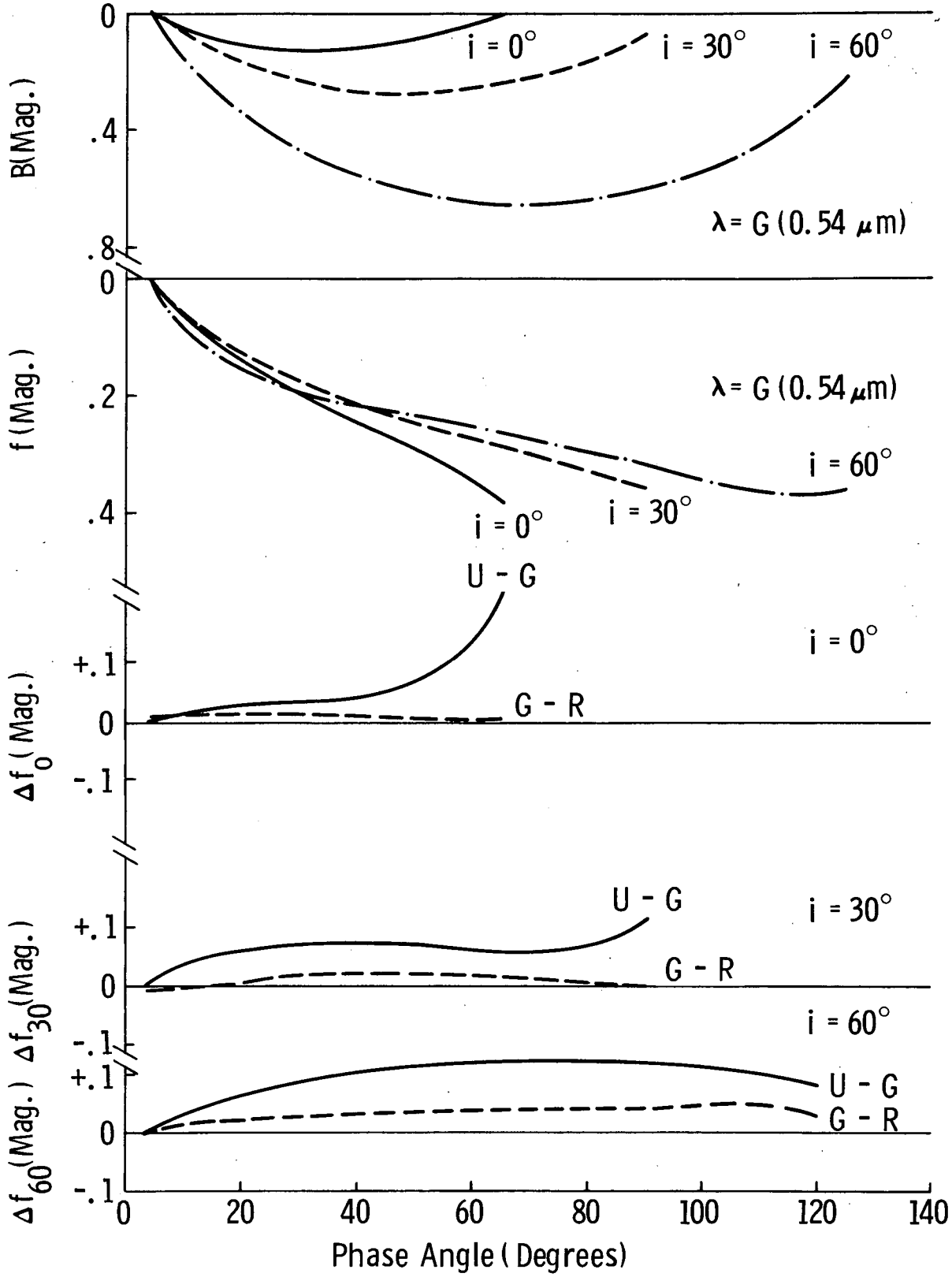

Fig. 6 Photometric Properties of < 37 μm Bruderheim Powder

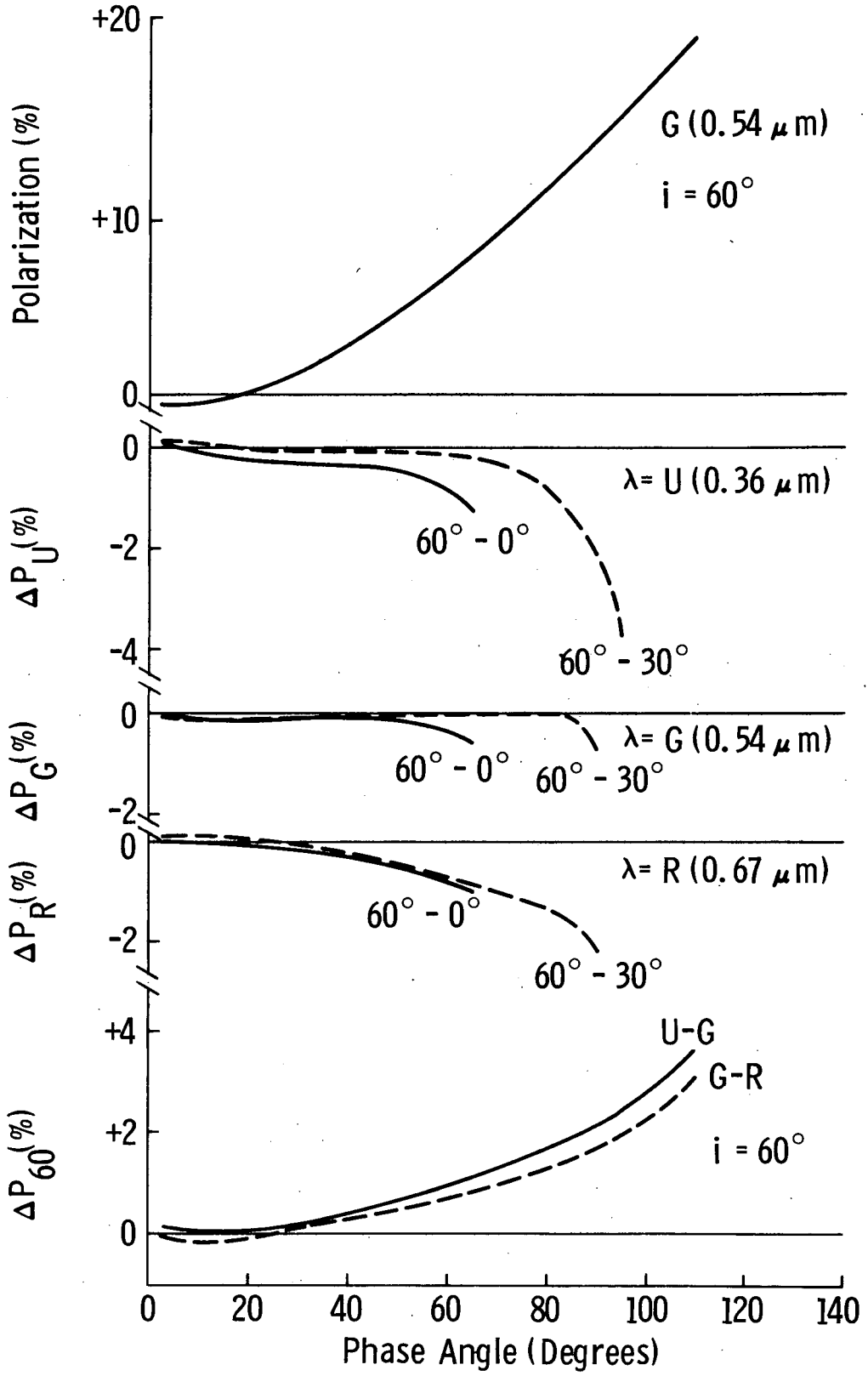

Fig. 7 Polarimetric Properties of 0.25 to 4.76 mm Bruderheim Particulates

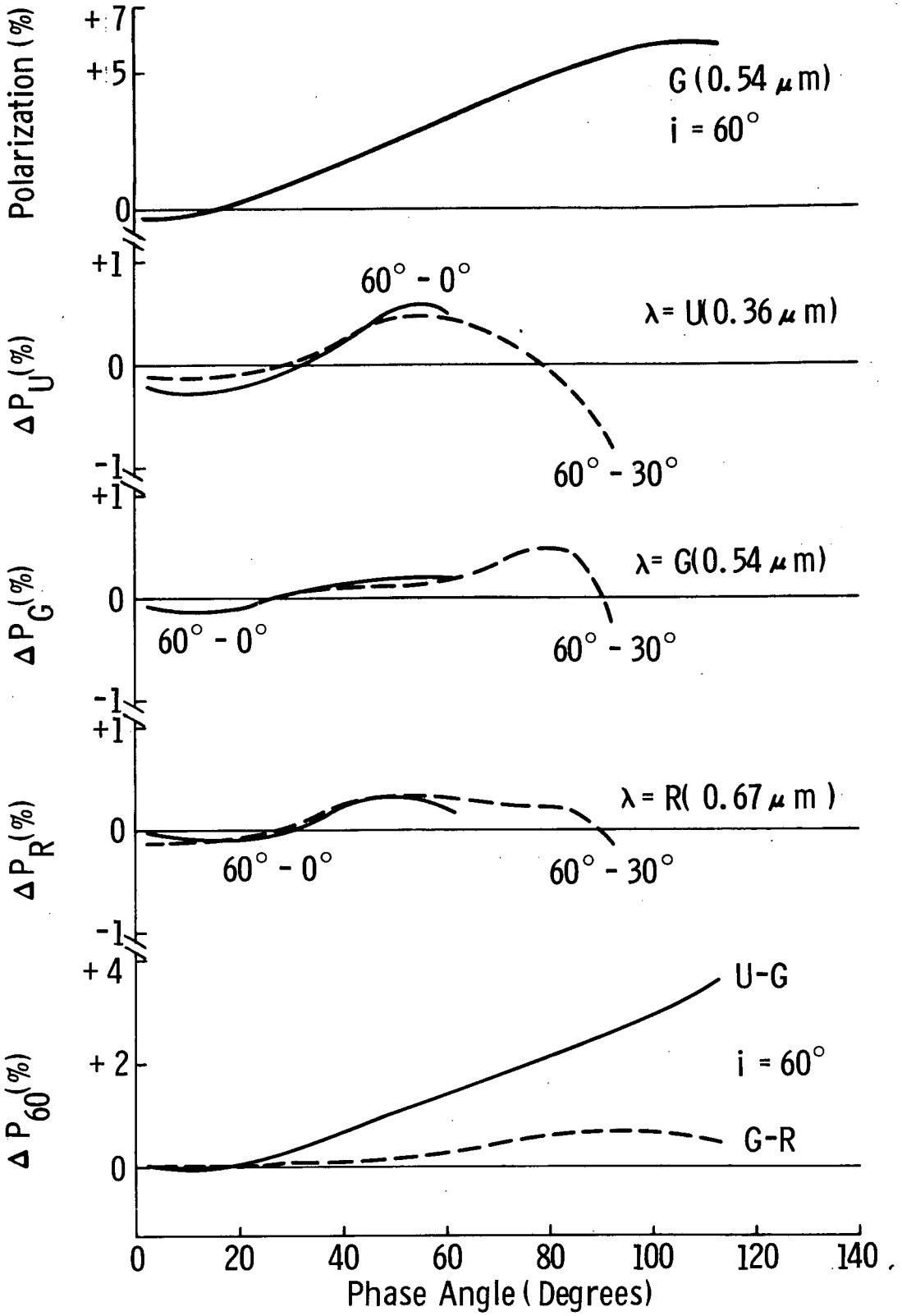

Fig. 8 Polarimetric Properties of 0.25 to 4.76 mm Bruderheim Particulates Coated with < 74 μm Bruderheim Powder

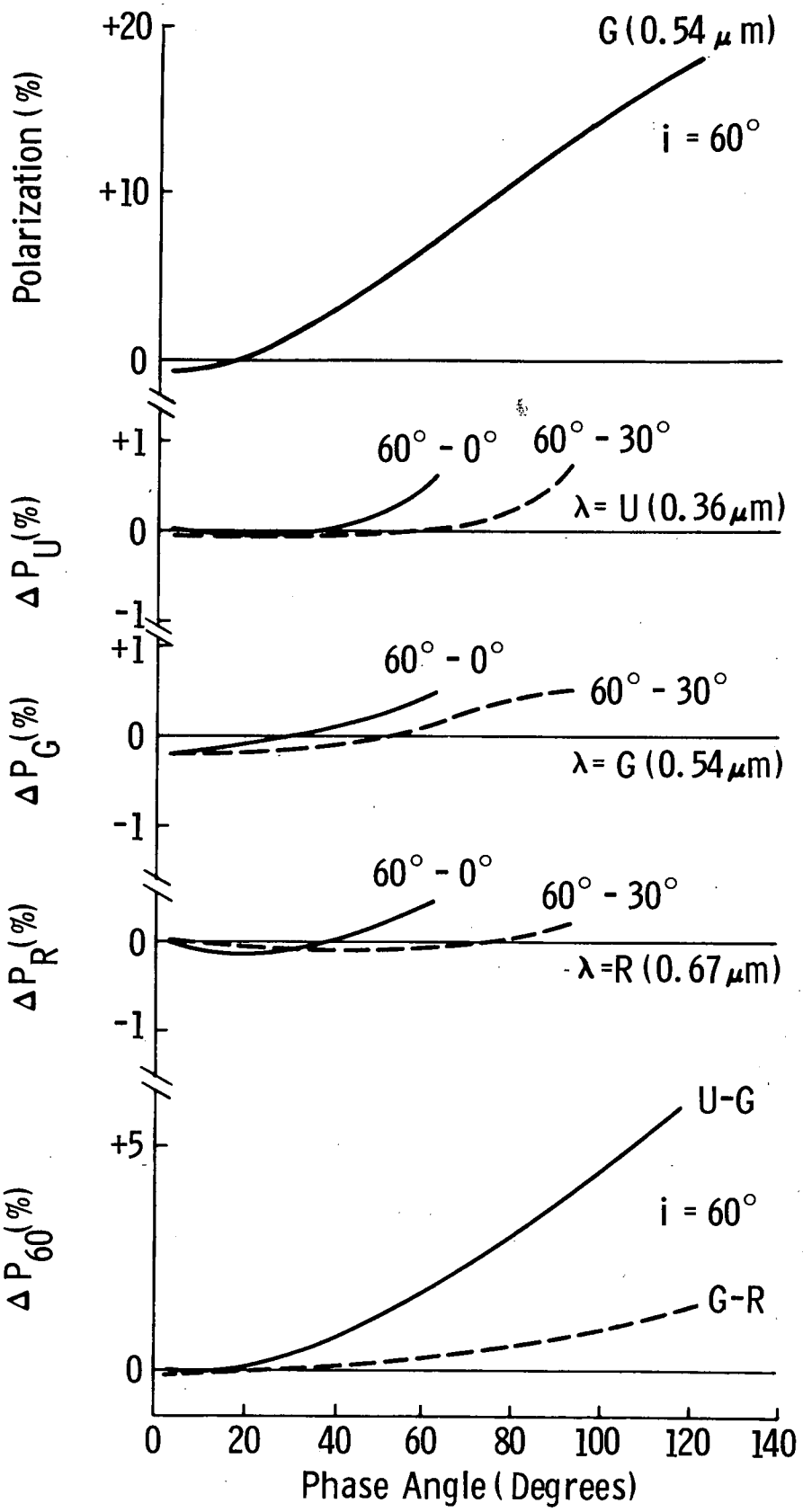

Fig. 9 Polarimetric Properties of 74 to 250 μm Bruderheim Grains

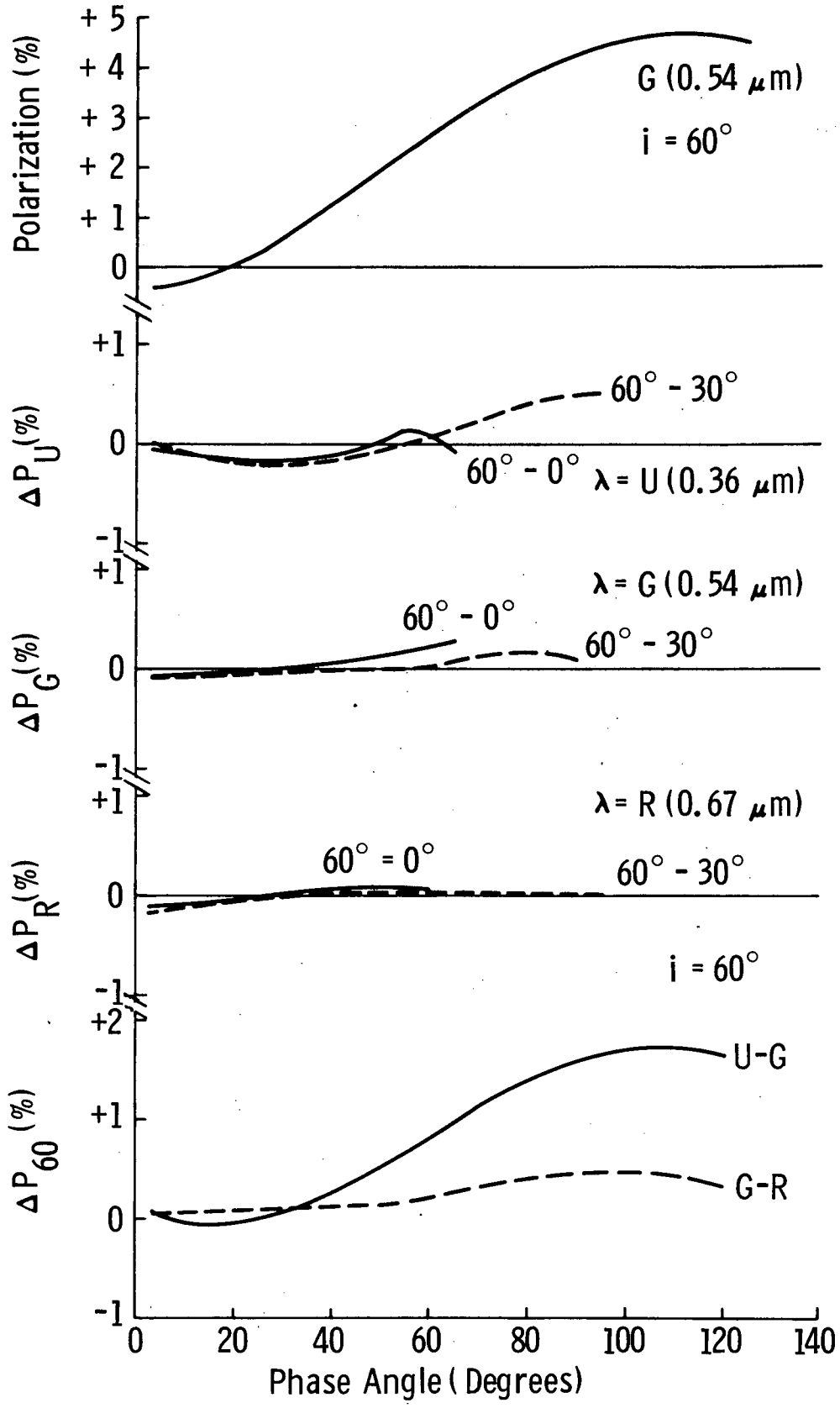

Fig. 10 Polarimetric Properties of < 37 μm Bruderheim Powder

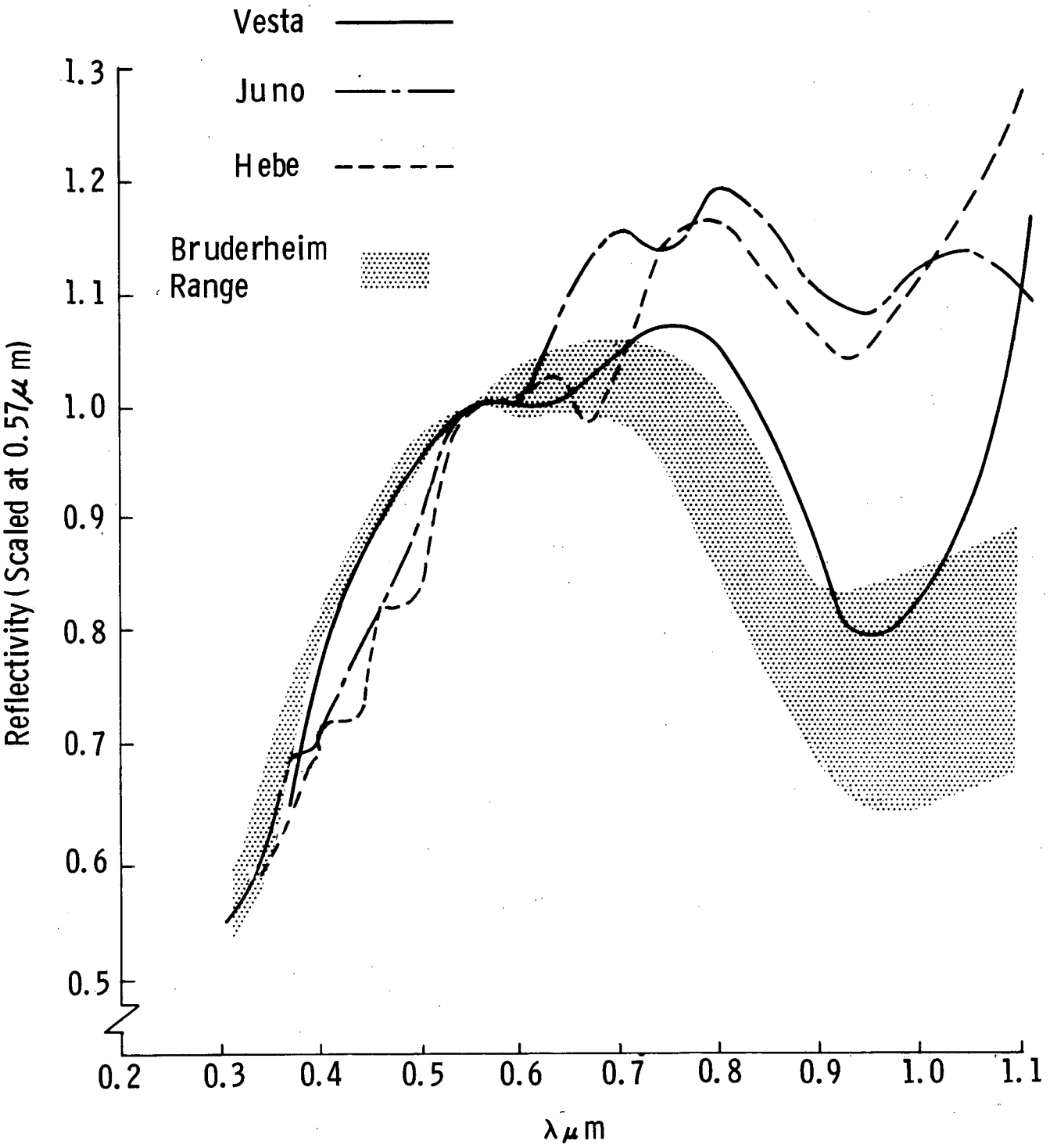

Fig. 11 Comparison of the Bruderheim Spectral Reflectance Curves with Those of Various Asteroids; the Curves Have Been Normalized to Unity at 0.56 μm
a) Vesta, Juno and Hebe (Chapman, 1972)

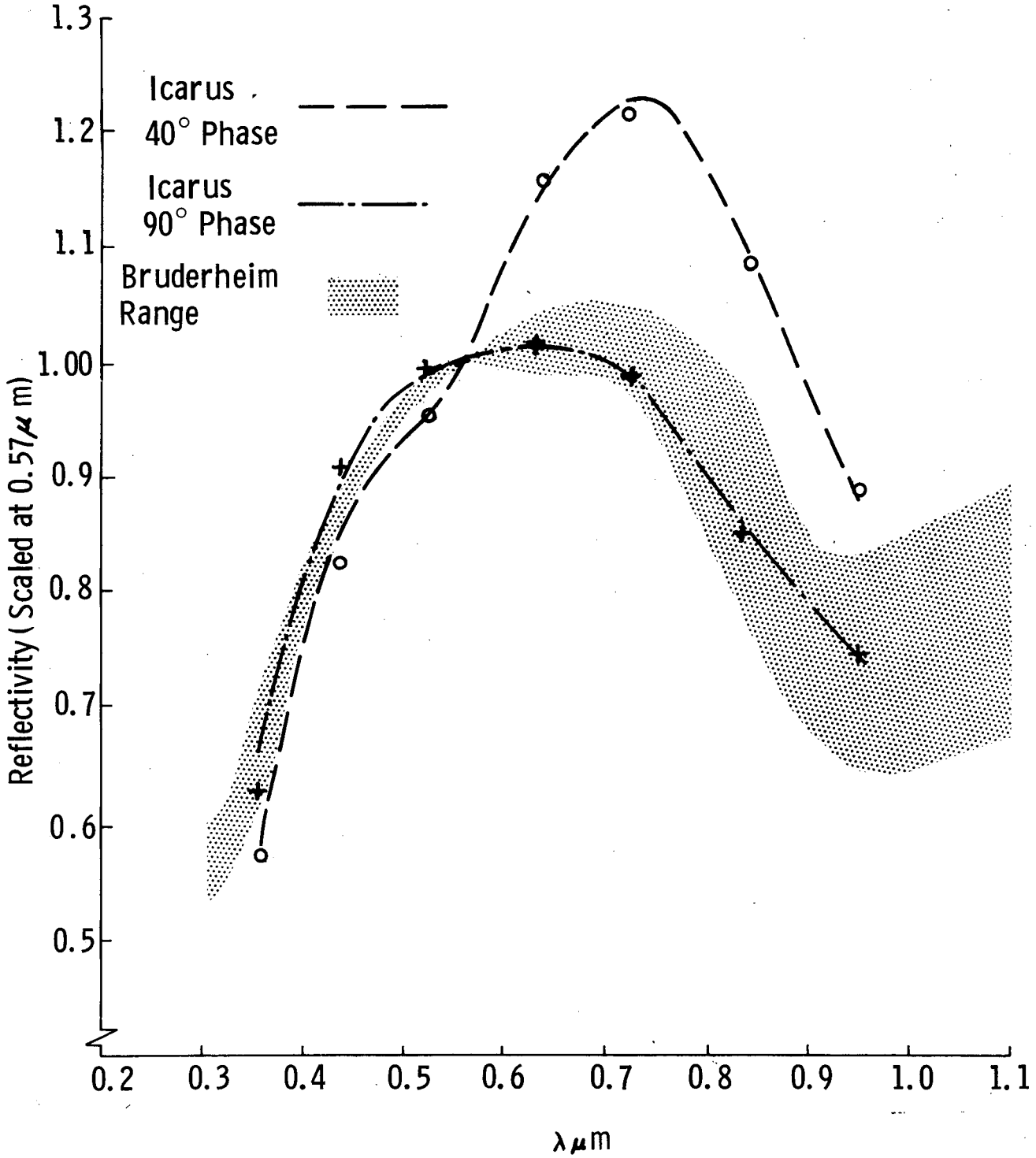

Fig. 11 (Cont.) Comparison of the Bruderheim Spectral Reflectance Curves with Those of Various Asteroids; the Curves Have Been Normalized to Unity at 0.56 μm
b) Icarus (Gehrels, 1970)